Egypt. J. Chem. **Vol. 64,** No. 4 pp. 1867 - 1876 (2021)

Egyptian Journal of Chemistry

http://ejchem.journals.ekb.eg/

Ionic Liquid as Water Soluble and Potential Inhibitor for Corrosion and Microbial Corrosion for Iron Artifacts

A. M. El-Shamy[a*], M. Abdelbar[b]

[a] *Physical Chemistry Department, Electrochemistry and Corrosion Lab., National Research Centre, El-Bohouth St. 33, Dokki, P.O. 12622, Giza, Egypt*

[b] *Conservation Department, Faculty of Archaeology, Damietta University, Damietta El-Gadeeda City, Damietta Governorate, 34511, Egypt*

Abstract

The interactions between the metal and its environment are responsible for the electrochemical reactions leading to corrosion. To avoid further degradation and in general the appearance of corrosion products, a corrosion inhibitor must be applied on the metallic surface to reduce or prevent the corrosion of exposed metal in a corrosive environment. Corrosion inhibitors are one of the different methods used by conservation-restoration professionals to preserve metallic cultural heritage. The present case study is concerned with preserve and controls the corrosion of the iron entrance door/gate of the clock tower of Muhammad Ali mosque at Salah Ed-din Cairo citadel- Egypt, by using an environmentally friendly Corrosion inhibitor. 1-butyl-1-pyrrolidinium chloride Ionic Liquid is of attentiveness since there has been a growth in ecological consciousness and a variation in guidelines that control the toxicity of systematic corrosion inhibitors. So, the natural products are becoming the main source of environmentally friendly corrosion inhibitors. Furthermost their extracts comprising the required features of the traditional corrosion inhibitors such as oxygen, carbon, nitrogen, and sulfur. These elements are contributed to the adsorption process on the metal surfaces and arrangement of a protective layer, which shields the metal surface against environmental corrosion. Progress of green chemical knowledge compromises a new artificial approach for ionic liquids. These compounds are well-thought-out as new safe corrosion inhibitors which act in different corrosive conditions. Finally, applications of vapor-phase inhibitors and their role of action are recommended in the protection of iron door under study.

Keywords: Conservation; Environmentally Friendly Inhibitors; Corrosion Control; Iron Artifacts; Ionic Liquid; Microbial Corrosion Inhibitors.

1. Introduction

The protection of metals or metal alloys from deterioration process could be approached by separating the metal structures from belligerent environment. This phenomenon could be happened by means of coatings or by forming a protected film by using chemical molecule or compensate for the release of electrons. However, the corrosion is considered as an oxidation of metallic structures since the corroded structure is formed. The corrosion control might be achieved by using organic and/or inorganic compounds. The mode of action of these inhibitors is comprises the adsorption of the chemical molecules on the metallic structure to segregate it from its adjacent environment to prevent the oxidation-reduction development by forming a thin protective layer [1]. Most of the famous corrosion inhibitors are toxic, so we must lead to the use of some new safe corrosion inhibitors. We call that the corrosion inhibitors are act perfect when they are added in low doses to care for the surface against corrosive atmosphere [2-6]. The exploit of inhibitors molecules happens owing to their adsorption process on the surface in the type of neutral particles as an alternative of hydrogen ions as described in the following equation.

*Corresponding author e-mail: elshamy10@yahoo.com.; (*A. M. El-Shamy*).

Receive Date: 22 September 2020, Revise Date: 28 December 2020, Accept Date: 03 January 2021

DOI: 10.21608/ejchem.2021.43786.2887

$$\text{Inhibitor} + n\,H_{ads} \rightarrow \text{Inhibitor}_{ads} + H_2 \quad (1)$$

This action prevents the most cathodic reactions as seen in the following equations:

$$2H^+ + 2e^- \rightarrow H_2 \quad (2)$$

$$O_2 + 4H^+ + 4e^- \rightarrow 2H_2O \quad (3)$$

$$2H^+ + 2e^- \rightarrow H_{ads} \rightarrow 2H_2 \quad (4)$$

Specific requirements and needs must be provided for using corrosion inhibitors in conservation treatments, including cost and amount, easy availability and most important safety to environment and its species, this can be achieved by using environmentally friendly inhibitors or green inhibitors. Green corrosion inhibitors are biodegradable and do not contain heavy metals or other toxic compounds. Over the years, great efforts have been employed to find suitable corrosion inhibitors of organic origin in various corrosive media [7-10]. The present case study is the iron door/entrance of the clock tower of Muhammad Ali mosque at Salah Ed-din Cairo citadel- Egypt. The clock tower was erected in 1845 AD, located in the western corridor of the courtyard of Muhammad Ali's mosque at Salah Ed-din Cairo citadel, and is a combination of Islamic and Gothic influences. The iron door was painted with orange and green coats Fig. 1 and Fig. 2, historically, ironworks have often been coated, not only for protection, but also to improve their appearance or to imitate other materials [11]. A small group of pigments - red lead, iron oxide, tar, and graphite - reappear constantly in 19th century discussions of metal primers [12]. The corrosion aspect of the gate was attributed to the failure of the old coating layer, where it has been broken, flaked and blistered. Therefore, it will trap and hold water to the iron, preventing it from drying out properly, pinholes in the coating allow the promotion of corrosion cells in which an anodic area develops under the film around the hole, causing corrosion to spread [13, 14]. When exposed to precipitation and oxygen in the atmosphere, iron undergoes oxidation to form iron oxide (commonly known as rust). Rust weakens the object and allows damage to underlying layers of metal [15]. Examination and analysis were carried out to identify the morphology and the elemental analysis of the iron alloy in the door to prepare iron coupons simulated to the composition and morphology of the iron alloy, which could be used all along our experimental work. Weight loss and electrochemical experiments were carried out on iron coupons to evaluate the efficiency of 1-butyl-1-pyrrolidinium chloride Ionic Liquid to protect the iron door/gate.

Fig. 1: shows the main entrance gate/door of the clock tower of Muhammad Ali mosque at Salah Ed-din Cairo citadel, Egypt, (1830 A.D).

Fig. 2: shows the iron was corroded due to paint detachment.

2. Materials and Methods

2.1. Materials

Documentation of the iron door has been undertaken using photographic recording. Examinations and analysis were conducted to identify the type of the iron alloy used, to identify methods of manufacturing and detecting the nature of corrosion products. This has been achieved by using metallographic microscopy, SEM with EDS, carbon-sulphur analyser and XRD. Metallographic examination was accomplished on un-etched polished cross section through an OLYMPUSU-PMTVC2D03043JAPAN metallographic microscope. The same sample was carefully investigated using JEOL model JSM-53000 scanning electron microscope (SEM) with energy dispersive spectrometer (EDS). The carbon and sulphur contents in the iron alloys used in the door/gate were determined using Carbon/Sulphur analyser ELTRA CS-2000. Sample weighing (0.5 gram) was taken from the iron alloy. The XRD analysis was undertaken with D8 advance X-Ray diffractometer X. (Bruker, Germany) to identifying corrosion products which formed on the iron surface.

2.2. Corrosion Techniques

Weight loss and electrochemical experiments were carried out on wrought iron of the following composition (wt. %): 0.19% C, 0.05% Si, 0.94% Mn, 0.009% P, 0.004% S, 0.014% Ni, 0.009% Cr, 0.034% Al, 0.016% V, 0.003% Ti, 0.022% Cu, and the rest Fe. Rectangular wrought iron coupons having dimensions of length 5.6, width 2.7, and thickness 0.5 cm with an exposed total surface area of 38.54 cm^2 were used for gravimetric measurements. For electrochemical experiments, the wrought iron cylinder, embedded in epoxy resin with an exposed surface area of 1 cm^2 to the electrolyte was used as working electrode with an exposed surface area of 1 cm^2. Before running all experiments, the surface of wrought iron was abraded with a series of emery paper (320-600-800-1000-1200) and then washed with bi-distilled water and acetone.

2.2.1. Test Solutions

Testing electrolyte was 3.5% NaCl solution diluted in distilled water, used as blank solution (corrosive medium). The inhibitor 1-butyl-1-pyrrolidinium chloride Ionic Liquid was purchased from Sigma Aldrich Co., and its chemical structure is presented in Fig. 3. The concentration range of IL used in this work was 25-500 ppm.

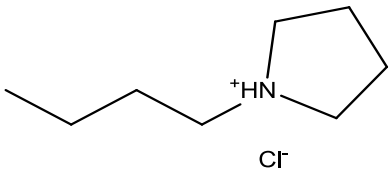

1-butyl-1-pyrrolidinium chloride

Fig. 3: The chemical structure of the studied ionic liquid as a corrosion inhibitor

2.2.2. Weight Loss Measurements

Weight loss tests were performed in a conical flask containing 100 ml of 3.5 % NaCl solution. Test samples were immersed in the flasks for 6 h at different temperatures ranging from 303-333 K. After immersion time the specimens were picked out, cleaned with distilled water, and dried. The differences of the weight of the specimens before and after immersion were recorded by digital electronic balance (sensitivity ± 0.1 mg). Inhibition efficiencies at different concentration of the IL (η_{WL}, %) were calculated from the following equation [16]:

$$\eta_{WL}, \% = \left(W_o - \frac{W}{W_o} \right) \times 100 \qquad (5)$$

$$\theta = W_o - \frac{W_o}{W} \qquad (6)$$

Where W_0 and W indicate weight loss in absence and presence of inhibitor respectively, and Θ is surface coverage value. From weight loss measurements, corrosion rates C_r (mg cm^{-2} h^{-1}), were calculated at various concentration of inhibitor with the help of following relation [16]:

$$C_r = \frac{\Delta W}{At} \qquad (7)$$

Where ΔW is weight loss of the sample in mg, A is area of the exposure in cm^2; t is immersion time in hours.

2.2.3. Electrochemical Studies

Electrochemical experiments were carried out using a Voltalab 40 Potentiostat PGZ 301 in a conventional electrolytic cell with three-electrode arrangement: saturated calomel reference electrode (SCE), a platinum wire as a counter electrode and the wrought iron as working electrode (WE). All measurements were conducted at 303 K. Potentiodynamic polarization curves were obtained by changing the electrode potential automatically (from –800 to –300 mV vs. SCE) at open circuit potential with a scan rate of 2 mV s^{-1}. Electrochemical impedance spectroscopy measurements were carried out using A Radiometer Voltalab Master 40 Type PGZ 301. Impedance spectra were obtained in the frequency range between 100 kHz and 50 mHz using 10 steps per frequency decade at the corrosion potential after 30 min. of immersion in test solutions without and with different concentrations of the prepared inhibitor. AC signal with 10mV amplitude peaks to peak was used to perturb the system. The data were analyzed using the Zsimpwin software program and EIS diagrams are given in the Nyquist representation. All experiments were performed in atmospheric condition without stirring at 303 K.

2.2.4. Surface Analysis

2.2.4.1. Scanning Electron Microscope (SEM)

It is necessary to know the morphological changes occurred on the wrought iron surface due to the corrosion process before and after the addition of inhibitors. To handle the demand, SEM was used. The specimens were first immersed in 1M HCl in the absence and presence of optimal concentrations (500 ppm) of the tested compounds for 48 hrs at room temperature, then taken out from the test solutions, cleaned with bi-distilled water and acetone, and dried with cool air. The SEM images were conducted using JEOL model JSM-53000 scanning electron microscope (SEM).

2.2.4.2. EDX

EDX analysis was performed with energy dispersive spectrometer conjugated with Jeol 5400 scanning electron microscope (SEM). Prior to analysis, the wrought iron specimens have been kept immersed in 3.5 % NaCl solution for 48h in absence and in the presence of 60 x 10^{-5} M of the inhibitor. Finally, the specimens have been washed thoroughly and submitted to 5 min of ultrasonic cleaning to remove loosely adsorbed ions.

2.2.4.3. X-Ray Diffraction Analysis (XRD)

wrought iron coupons were immersed in 3.5 % NaCl solution for 48 hrs in absence and presence of optimum concentration of the studied inhibitor. The corrosion products developed on the surface of the coupons were taken up, gently powdered and homogenized. The identification of the phases was carried out using X-ray powder diffractometer, X'PERT PRO MPD (PANalytical, Netherland). The XRD patterns were recorded with a Cu Kα radiation of wavelength of 1.5406 Aº operated at 40 kV/40 mA. The samples were step-scanned in the 2θ range of 4º-80º with a step size 0.02 and a time step of 0.4s. The individual crystalline phases formed on the wrought

iron surface were identified using the ICDD-PDF database.

2.3. Microbial Corrosion Measurements

The ionic liquid 1-butyl-1-pyrrolidinium chloride (Io.Li.Tec., Germany) with purity of 99% was used as received without further purification or drying. Serial dilution method is used to enumerate the existed microorganisms in circulating water. One of the best benefits the most probable number (MPN) method, is the counting is occurred only for the live cells of microorganisms. The samples are collected from the circulating water system as follows: First, the water sample was subjected to circulation in open air for 24h to enrich the planktonic bacterial growth then; 1 ml from circulating water was used to detect the bacterial counts before ionic liquid injection. The circulating water was injected by different concentrations of ionic liquids. Synthetic Postgate media were used and distributed in test tubes, each tube contained 9 ml, and 6 sterilized tubes were used for each MPN experiment. The circulated water was used to determine the biocidal efficiency of the employed ionic liquid through injection of the IL with different doses and then 1 ml from each treatment was used to inoculate in the first sterilized tube. Afterward, the tube was shaking well and then 1 ml was withdrawn and injected in the second tube and the same was done with the other tubes. The tubes used for the MPN analysis were incubated at 30° C. For sessile bacteria, the water was circulated for 3 days. After the first day the population of planktonic bacteria was more than, 100,000 colony/ml. A mild steel coupon of area 1×1 cm^2 was then immersed in the medium and the bacteria started to settle on the surface in the second and third days, forming a biofilm. The obtained biofilm was removed by sonication of the steel sample in a sonicator for 10 s in sterile water then, samples from water were used to detect the bacterial counts by using the serial dilution method as mentioned above for planktonic bacteria. All steps were repeated with different concentrations of the employed ionic liquid to show its effect on the sessile bacteria [17, 18].

3. Results and Discussions

3.1. Characterization of The Iron Door

Un-etched sample was examined under metallographic and SEM with EDS to identify the type of iron alloy used in manufacturing the iron decorations as presented in Fig. 4 and 5.

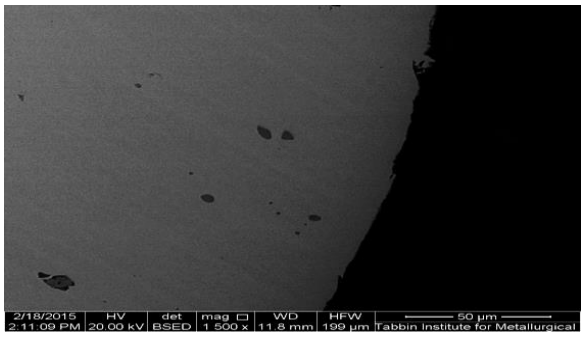

Fig. 4: shows metallographic image of the iron alloy.

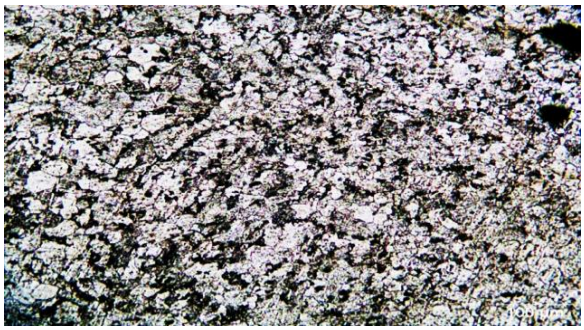

Fig. 5: SEM image shows the surface morphology of the iron alloy.

A corroded sample was examined under SEM/EDS as shown in Fig. 6. EDS analysis of the iron alloy showed 68.22% iron and 32.64% oxygen. By using Carbon/Sulphur analyser, it has been shown that the alloy contains 0.195%wt carbon and 0.15 wt % Sulphur.

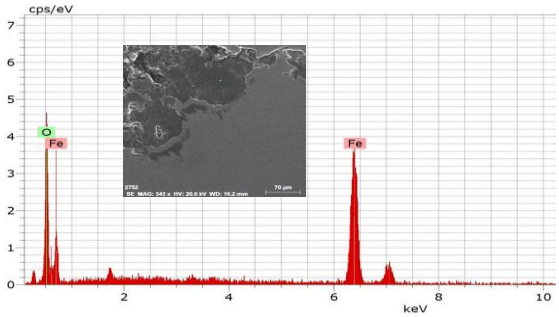

Fig. 6: show SEM image of corrosion products covered the iron surface and the corresponding EDS analysis showing a spot analysis of the iron surface.

The corrosion products which formed on the iron surface were identified using x-ray diffraction as shown in Fig. 7 and Table 1. Through the above-mentioned results, the iron alloy used in the iron decorations is wrought iron, where the main forms of iron alloys used throughout history are cast iron, wrought iron and steel. Wrought iron contains little carbon (not more than 0.35 %), steel has a moderate carbon content (between 0.6% and 2 %) and cast irons have a high carbon content greater than 2% but

generally less than 5% [19-21]. Wrought iron was largely used in Decorative ironwork until the latter half of the 18th century, when cast iron became increasingly and the demand for mass-production [22]. Fences, gates, railings, and balconies have been traditional architectural uses of wrought iron [23]. The microstructure of wrought iron is easily recognized, consisting primary of ductile α–iron (ferrite) matrix with slag inclusion (a glassy material that is deliberately added or worked into the iron during manufacture), mostly FeO and SiO_2 [24, 25]. Wrought iron melts at 1535°C and is remarkably malleable and generally ductile (unless it has been overworked and not annealed by re-heating), with similar strengths in tension and compression. The more wrought iron is worked the stronger it becomes [26].

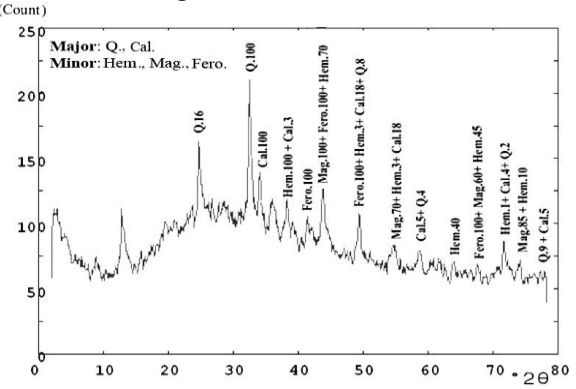

Fig. 7: shows XRD pattern of the corrosion products that formed on the iron surface.

Corrosion products identified by XRD analyses composed of Hematite (Fe_2O_3), Feroxyhite FeO(OH) and Magnetite (Fe_3O_4). Dust particles can be also recognized which include Quartz (SiO_2) and Calcite ($CaCO_3$) accumulated above the corrosion layers. Iron exposed to the atmosphere develops a moderately protective film of oxides and hydroxides forms [27]. There is an inner layer of magnetite along with other amorphous iron corrosion products, and an outer layer of iron hydroxide oxides [28].

3.1. Weight loss measurements

The weight loss method is the most used methods to evaluate inhibition efficiency of any inhibitor due to the simplicity and reliability of its measurements. The values of corrosion rate C_r (mg cm^{-2} h^{-1}), the surface coverage (Θ) and the inhibition efficiency η_w (%) obtained from weight loss measurements for wrought iron after (6h) of immersion in 3.5 % NaCl solution with and without the addition of different concentrations of the tested inhibitor at various temperatures 303,313,323 and 333 K is shown in Table 2. The results illustrate the effects of ionic liquid inhibitor on corrosion rate and inhibition efficiency as a function of inhibitor concentration. The rate of wrought iron dissolution was lowered, while inhibition efficiency increased with increase in inhibitor concentration. The corrosion rate (C_r) and inhibition efficiency data obtained from weight loss measurements are depicted in Table 2.

It is clearly shown from these values that decreasing the weight loss values were leading to suppression of the corrosion rate and increasing the surface coverage area with increasing in inhibitor concentration and the ionic liquid compound is significantly effective against corrosion in sodium chloride solution, which suggested that the adsorption of this compound onto the wrought iron surface from chloride solutions [29-32].

Table 1: shows results of XRD analysis of corrosion products that formed on the iron surface.

Samples	***Compounds***	
	Major	***Minor***
Corrosion products	Quartz SiO_2 (29.81%) Calcite $CaCO_3$ (21.80%)	Feroxyhite FeO(OH) (18%) Magnetite Fe_3O_4 (15.33%) Hematite Fe_2O_3 (15.04%)

Table 2: Weight loss data for wrought iron in 3.5% NaCl without and with different concentrations of the ionic liquid compound at various temperatures

Conc., ppm	***303 K***			***313 K***			***323 K***			***333 K***		
	C. R, mg.cm^{-2} h^{-1}	***θ***	***I.E, %***	***C. R, mg.cm^{-2} h^{-1}***	***θ***	***I.E, %***	***C. R, mg cm^{-2} h^{-1}***	***θ***	***I.E, %***	***C. R, mg cm^{-2} h^{-1}***	***θ***	***I.E, %***
3.5% NaCl	0.006	--	--	0.010	--	--	0.016	--	--	0.026	--	--
25	0.001	0.81	80.8	0.002	0.82	82	0.003	0.83	83.1	0.004	0.84	83.9
50	0.001	0.84	83.6	0.0015	0.86	85.6	0.002	0.87	87.4	0.003	0.89	87.8
100	0.0007	0.89	88.7	0.001	0.91	90.8	0.001	0.93	92.5	0.0015	0.94	93.8
150	0.0005	0.93	92.6	0.0006	0.95	94.5	0.0007	0.96	95.9	0.0008	0.97	95.7
200	0.0002	0.97	97.2	0.0002	0.98	98.1	0.0002	0.99	98.7	0.0002	0.99	98.6

3.2. Electrochemical Measurements

3.2.1. Potentiodynamic Polarization Curves

Potentiodynamic anodic and cathodic polarization plots for wrought iron in 3.5% NaCl solution, in absence and in the presence of different concentrations of ionic liquid 1-butyl-1-pyrrolidinium chloride are shown in Fig. 8. This figure shows that the anodic and cathodic reactions are affected by the ionic liquid. It means that the addition of 1-butyl-1-pyrrolidinium chloride reduces the anodic dissolution of wrought iron and retards the cathodic hydrogen evolution reaction. These results indicated that this inhibitor exhibits cathodic and anodic inhibition effects. The respective kinetic parameters including corrosion current density (I_{corr}), corrosion potential (E_{corr}), cathodic Tafel slope (β_c), anodic Tafel slope (β_a), corrosion rate (µm/Y) and inhibition efficiency (η %) are given in Table 3. The inhibition efficiency (η %) was calculated from the corrosion current density using the following equation [33]:

$$\eta_{Tafel}, \% = \left(i - \frac{i}{i_o} \right) \times 100 \qquad (8)$$

Where i_o and i are the corrosion current density values in the absence and presence of alkaloids extract, respectively. According to the obtained results, the inhibition efficiency of IL increases with inhibitor concentration, reaching a maximum value at 500 ppm. This behavior shows that IL acts as effective inhibitor for the corrosion of wrought iron in 3.5% NaCl media. The cathodic Tafel slope (βc) and the anodic Tafel slope (βa) of IL changed with inhibitor concentration. This observation suggests that the inhibitor molecules controlled the two reactions and adsorbed on the metal surface by blocking the active sites on the metal surface, retarding the corrosion reaction [34]. Also, the corrosion potential (E_{corr}) shifts slightly towards more negative and positive potential in the presence of inhibitor, suggesting that the mechanism of inhibitor adsorption over the metal surface obeys the adsorption phenomenon that hinders both anodic and cathodic reactions. The value of E_{corr} displacement was less than 85 mV and because this inhibitor reduces the cathodic and anodic current densities, it is likely that IL acts as a mixed-type inhibitor with predominantly cathodic type [35].

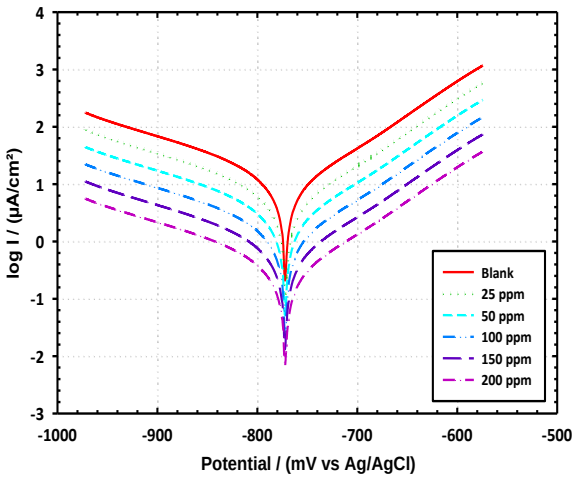

Fig. 8: Polarization plots of carbon steel electrode obtained in 3.5 wt % NaCl solution and containing various concentrations of IL at 298 K.

This could be explained based on inhibitor adsorption on the metal surface and the adsorption process enhances with increasing inhibitor concentration. In addition, the cathodic current potential curves Table 3 gave rise to parallel lines indicating that the addition of IL to the 3.5 % NaCl solution did not modify the hydrogen evolution mechanism and the reduction of H^+ ions at the wrought iron surface takes place mainly through a charge transfer mechanism. The inhibitor was first adsorbed on the wrought iron surface and blocked the reaction sites of the wrought iron surface. In this way, the surface area available for H^+ ions were decreased while the actual reaction mechanism remains unaffected [36].

Table 3: Polarization parameters and the corresponding inhibition efficiencies for the corrosion of wrought iron in 3.5 % NaCl containing different concentrations of IL compound at 303 K

Conc., ppm	*E, mV*	*i_{corr} µA.cm^{-2}*	*B_a mV*	*B_c mV*	*CR µm/Y*	*θ*	*I.E., %*
3.5% NaCl	-761	0.030	102	-107	346	---	----
25	-772	0.006	109	-118	69	0.80	78.4
50	-781	0.006	199	-129	62	0.82	79.1
100	-798	0.004	210	-131	46	0.86	85.2
150	-812	0.003	222	-136	36	0.89	88.8
200	-821	0.001	277	-138	18	0.95	94.9

Table 4: Electrochemical impedance parameters for the corrosion of wrought iron in the absence and presence of different concentrations of Schiff base derivatives at 303 K.

Conc., ppm	R_s	*CPE* $S.s^n/cm^2$	*n*	R_p $\Omega.cm^2$	C_C mF/cm^2	*CPE* $S.s^n/cm^2$	*n*	R_{ct} $\Omega.cm^2$	C_{dl} mF/cm^2	*I.E, %*
3.5% NaCl	12	0.0015	0.63	277	0.99	0.0016	0.78	357	1.455	-----
25	14	0.0008	0.74	960	0.81	0.0011	0.82	1115	1.042	28.4
50	16	0.0008	0.75	1094	0.76	0.0007	0.89	2320	0.812	44.2
100	17	0.0002	0.79	1164	0.62	0.0005	0.92	2460	0.652	55.2
150	18	0.0005	0.83	1260	0.53	0.0003	0.94	2866	0.324	77.7
200	19	0.0005	0.84	1363	0.41	0.0001	0.96	3218	0.166	88.5

3.2.2. Electrochemical impedance spectroscopy

Electrochemical impedance spectroscopy was used to examine the inhibition efficiencies of IL compound on wrought iron in 3.5 % NaCl solution. The electrochemical impedance diagram of wrought iron in 3.5 % NaCl solution in the absence and presence of five different concentrations of IL compound was depicted in Fig. 9 and Table 4. The impedance spectra were given in Nyquist representation.

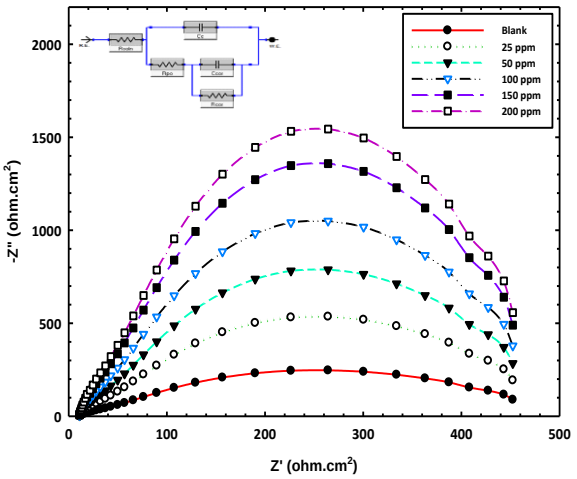

Fig. 9: Nyquist plots and electrochemical circuit model of carbon steel electrode obtained in 3.5 wt % NaCl solution and containing various concentrations of IL at 298 K.

3.3. Microbial Corrosion Results

The inspiration of the ionic liquid on the planktonic bacterial progress was inspected. Fig. 10 displays the degeneration of the microbial counts with period at diverse loads of ionic liquid. As realized, at 25 ppm the bacteriological counts apparently decline by time and a comprehensive effect is accomplished afterward 7 h. As the IL load upsurges the rate of microbial progress effect upsurges and afterward 1h of the experiment, the bacteriological counts are condensed beginning around, 10^6 colony/ml to fewer than 10^5, 10^4, 10^3, 10^2 and 10 colony/ml at IL loads of 25, 50, 100, 150 and 200 ppm, correspondingly. Total effect is gotten afterward 6, 5, 4, 3, 2 and 1h at loads of 25, 50, 100, 150 and 200 ppm, individually. This designates that, the bactericidal impression of IL, and the inhibition rate is reliant on the IL load. The consequence of the working IL on sessile microorganisms was also inspected. As recognized, microorganisms are originated in two separate circumstances either permitted fluctuating in aqueous media which is called planktonic or involved in attached layer on the exterior super facials creating microbial biofilms which is called sessile. The planktonic microorganisms are extra inclined to the possessions of the biocides; but sessile bacteria display sophisticated fighting as they are frequently implanted in a self-produced polymeric matrix inside the microbial biofilm. Consequently, it is so hard to execute sessile than planktonic microorganisms owing to the difficult procedure of dissemination the microbial biofilms. It was described that, the required doses to execute the sessile microorganisms may be 600–700 ppm which, is greater than those mandatory to execute planktonic microorganisms in the similar types. Hereafter, the employ of distinctive research laboratory on planktonic microbes for assessment of the antiseptic competence of the IL, with the sake of governing the microbial corrosion, is not plentiful. Then, the antiseptic outcome of the working IL on sessile microorganisms was also considered. Fig. 10 displays the impact of IL by means of capricious loads on the self-consciousness efficacy of mutually planktonic and sessile microbes. The effectiveness of the bacteriological progress inhibition was assessed conferring to the succeeding formulary:

$$\text{I.E, (\%)} = \text{a-b/a X 100} \qquad (9)$$

Where a and b are the microbial counts without and with IL, individually.

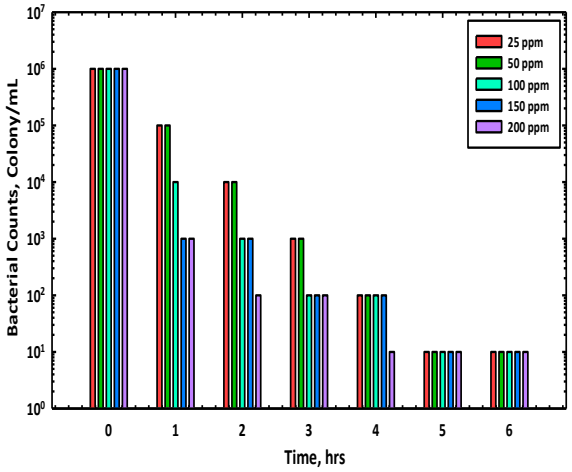

Fig. 10: The decline of bacteriological counts with time at diverse loads of the IL

As publicized in Fig. 11, for individually planktonic and sessile microorganisms, the inhibition effectiveness upsurges by the up surging in IL loads, and at one and the same load the hang-up efficacy of planktonic is always greater than that of sessile. At 25 ppm, the inhibition efficacy of planktonic and sessile bacteria was found to be 42 and 28%, separately, and it touched 96 and 68% at load of 300 ppm. It can be specified that, the working IL shows great inhibition efficacy against planktonic microorganisms and moderately low-slung loads of a few hundreds of ppm are required to realize total bacteriological embarrassment. Nevertheless, related with planktonic microbes, higher IL loads are desirable, around 2–3 times of extent, for sessile microorganisms to contract the similar effectiveness. According to these outcomes, it can be itemized that, the working IL can be stared as an effective biocide against aerobic and anaerobic bacteria.

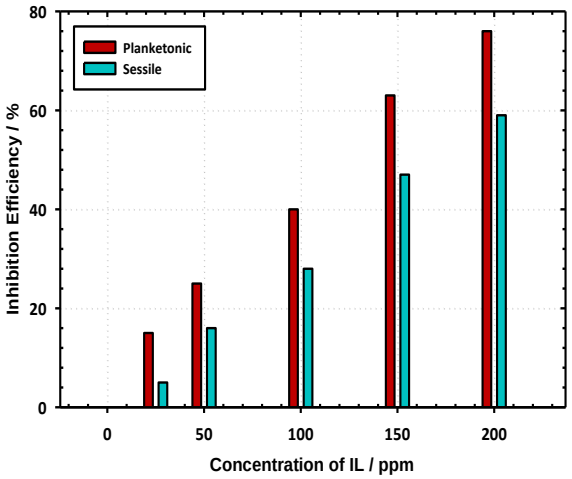

Fig. 11: The effect of IL's loads on the inhibition efficiency of bacterial growth for planktonic and sessile bacteria.

3.3. Conservation Process

Based on the results of the analytical data, the restoration interventions involved cleaning of the rusted surface through different methods, like wire brushing e.g., to remove the old paint, this is because the corrosion under the paint layers would potentially reactivate as soon as the clear topcoat began to fail, causing more rapid corrosion overall, and the poor adherence of any topcoat to a failing and irregular paint layer would speed this inevitable process significantly [37]. Thorough surface preparation is necessary for the adhesion of new protective coatings. All loose, flaking, and deteriorated paint must be removed from the iron, as well as dirt, oil, and grease. Old paint that is tightly adhered may be left on the surface of the metal if it is compatible with the proposed coatings. The retention of old paint also preserves the historic paint sequence which is essential for establishing the artistic technique used by the artist [38]. In general, the usual approach in the past has been the complete removal of the overlying paint layers, and finally re-coating with two or three layers of a protective material [39]. The preferred decision in this case study is to preserve the paint layers that well adhered to the iron surface and remove all loose, flaking, and deteriorated paints to prepare the surface to receive the new coating to guarantee the complete protection of the iron surface.

4. Conclusion

The influence of the ionic liquid 1-butyl-1-pyrrolidinium chloride on the bacterial growth inhibition and on the corrosion inhibition of wrought iron in 3.5% NaCl solutions was studied. It was found that the employed ionic liquid can be regarded as a dual function inhibitor for the bacterial growth and for the corrosion of wrought iron in 3.5% NaCl solutions. The results show that relatively low concentrations of 1-butyl-1-pyrrolidinium chloride can effectively inhibit the planktonic bacterial population. However, compared with planktonic bacteria, higher IL concentrations are needed, about 2–3 times, for sessile bacteria to get the same inhibition efficiency. The potentiodynamic polarization and impedance spectroscopy results reveal the anticorrosion influence of the employed ionic liquid. The corrosion inhibition was achieved by adsorption of the ionic liquid species onto the wrought iron surface forming a protective film against corrosion attack. The most important conservation step of metal artifacts is the protection process, therefore, applications of 1-butyl-1-pyrrolidinium chloride is recommended in the protection of iron door under study.

5. Conflicts of interest

"There are no conflicts to declare".

6. Formatting of funding sources

No funding sources in this paper

7. Acknowledgments

The authors are greatly thanks to Prof. Dr. Mohamed Megahed Fayoum University for helping in discussion of these results.

8. References

[1] Hefter G. T., North N. A., Tan S. H., Corrosion. 53 (8): 657-667 (1997).
[2] Bethencourt M., Botana F. J., Calvino J. J., Marcos M., Rodriguez Chacon M. A., Corrosion Science. 40 (11): 1803-1819 (1998).
[3] Sabirneeza A. A. F., Geethanjali R., Subhashini S., Chemical Engineering Communications. 202 (22): 232-244 (2015).
[4] Branzoi F., Branzoi V., Licu C., Materials and Corrosion—Werkstoffe und Korrosion. 65 (6): 637-647 (2014).
[5] Singh P., Srivastava V., Quraishi M. A., Journal of Molecular Liquids. 216 (1): 164-173 (2016).
[6] Sanatkumar B. S., Nayak J., Shetty A. N., International Journal of Hydrogen Energy. 37 (11): 9431-9442 (2012).
[7] Rocca E., Mirambet F., 48. Woodhead, Cambridge, 308–334 (2007).
[8] Cano E., Lafuente D., European Federation of Corrosion (EFC) Series, (2013) 570-594.
[9] Popov B. N., 1st Ed., Elsevier, 581-597 (2015).
[10] Amitha Rani B. E. Basu B. J., International Journal of Corrosion Volume 2012, Article ID 380217: 1-15 (2012).
[11] Scott D. A., Eggert G., London: Archetype Publications, 145-147 (2009).
[12] Hawkes P. W., Bulletin of the Association for Preservation Technology, 11(1): 18 (1979).
[13] Wallis G. Bussell M., 123-159 (2008).
[14] Davey A., Historic Scotland (2013).
[15] Church J., Muto A., Striegel M., In: Hyslop E., Gonzalez V., Troalen L., Wilson L. (eds), Metal 2013: Proceedings of interim meeting of the ICOM-CC metal working group, Edinburgh, Scotland, 173 (2013).
[16] Khalid I. Kabel, Khaled Zakaria, Mohamed A. Abbas, E. A. Khamis. J. Ind. Eng. Chem. 23: 57-66 (2015).
[17] El-Shamy A. M., Soror T. Y., El-Dahan H. A., Ghazy E. A., Eweas A. F., Materials chemistry, and physics 114: 156-159 (2009).
[18] Neelam Garg and Abhinav Aeron., 337-362 (2014).
[19] Scott D. A., The J. Paul Getty Museum, Los Angeles (1991).
[20] Gayle, M., Look, D. W. and Waite, J. G., U.S. Department of the Interior (1992).
[21] *Taylor J. Wrought Ironwork, (*2000).
[22] Mitchell D. Ornamental Cast Iron, (2009).
[23] Alkhrafi, F. M. El-Shamy A. M., Ateya B. G., Int. J. Electrochem. Sci. 4: 1351–1364 (2009).
[24] Elban W. L., Borst M. A., Roubachewsky N. M., Kemp E. L., Tice P. C., West Virginia, Association for Preservation Technology, 29: 27-34 (1998).
[25] Bramfitt B. L. Benscoter A. O., USA (2002).
[26] Bussell M., In: Forsyth M. (eds), Blackwell Publishing Ltd, 173-191 (2007).
[27] Scott D. A., Eggert G., London: Archetype Publications, 145-147 (2009).
[28] Selwyn, L. Metals and Corrosion: A Handbook for Conservation Professional", Canadian Conservation Institute, Ottawa (2004).
[29] Shehata M. F., El-Shamy A. M., Zohdy K. M., Sherif E. S. M., Zein El Abedin S., Applied Sciences 10 (4): 1444–1453 (2020).
[30] Zohdy K. M., El-Shamy A. M., Kalmouch A., Gad E. A. M., Egypt. J. Petroleum 28: 355–359 (2019).
[31] Yuce] A. O., Kardas G., Corros. Sci. 58: 86–94 (2012).
[32] de Andrade J. S., Vieira M. R. S., Oliveira S. H., de Melo Santos S. K., Urtiga Filho S. L., Mater. Chem. Phys. 241: 122296 (2020).
[33] El-Shamy A. M., Gaballah S. T., El Meleigy A. E., International Journal of Recent Development in Engineering and Technology, 1 (2): 11-18 (2013).
[34] Ateya B. G., Alkharafi F. M., El-Shamy A. M., Saad A. Y., Abdalla R. M., J. Appl. Electrochem., 39: 383–389 (2009).
[35] El-Shamy A. M., Zohdy K. M., Journal of Applied Chemical Science International 2 (Issue: 2): 56-64 (2015).
[36] El-Shamy A. M., Shehata M. F., Samir T. Gaballah, Eman A. Elhefny., Journal of Advances in Chemistry 11 (2): 3441-3451 (2015).
[37] Gillies J. C., Seyb I., In: Hyslop E, Gonzalez V, Troalen L, Wilson L (eds), Metal 2013: Proceedings of interim meeting of the ICOM-CC metal working group, Edinburgh, Scotland, 153 (2013).
[38] Sherif E. M., Abbas A. T., Gopi D., El-Shamy A. M., J. Chem. 2014: 538794 (2014).
[39] Sherif E. M., Abbas A. T., Halfa H., El-Shamy A. M., Int. J. Electrochem. Sci. 10: 1777–1791 (2015).